International Journal of GEOMATE, Jan., 2018 Vol.14, Issue 42, pp. 65-70
Geotec., Const. Mat. & Env., ISSN:2186-2990, Japan, DOI: https://doi.org/10.21660/2018.42.7168

OPTIMUM USE OF GEOGRID IN THE UNBOUND GRANULAR LAYER FOR THE PAVEMENT CONSTRUCTION

*Aung Aung Soe[1], Jiro Kuwano[1], Ilyas Akram[1] and Takaya Kogure[1]

[1]Department of Civil and Environmental Engineering, Saitama University, Japan

*Corresponding Author, Received: 10 Jun. 2017, Revised: 17 Aug. 2017, Accepted: 21 Sept. 2017

ABSTRACT: The benefits of using geogrid for the pavement construction have been reported by many researchers. The well-known benefits are base course reduction and rut-depth reduction. Currently, the available information is still limited for the geogrid-stabilized pavement construction. In this study, the benefits of geogrid stabilization were investigated through series of laboratory test. Base-course thickness and reinforcement position of geogrid were considered as the control parameters and their influences were analyzed on the surface and subgrade deformations. The tests were performed in a rigid square-tank, and the subgrade and base course were modelled by using the fine and coarse silica sands. Triangular geogrid was used for the reinforcement. Cyclic loading was applied with the variable steps of loading ranging from 100 kPa to 550 kPa. From the test results, it was realized that the surface deformation was mainly contributed from the subgrade deformation in the thin base-course sections. In contrast, the base-course deterioration dominated and resulted in severe surface deformation in the thick base-course sections. This severe deformation was effectively reduced when geogrid location was shifted to the upward position inside base course layer. However, this geogrid position has negligible influence on the subgrade deformation, which is considerably affected by the base-course thickness. In all test cases, a progressive loss in base course thickness was noticed under high footing pressure. This loss is smaller in the thin section, compared to thick one. Test results revealed that the benefit of geogrid stabilization is more obvious in the thin section.

Keywords: Pavement, Base Course, Subgrade, Deformation, Geogrid Position

1. INTRODUCTION

Geosynthetic materials have been widely used in the geotechnical engineering applications due to their beneficial improvements. Depending on the applications and purposes, there are several types of geosynthetic materials, such as geocell, geotextile and geogrid. Among them, geotextile and geogrid are mainly applied in the flexible pavement constructions in order that the design service life of pavement could be extended and/or the amount of base course materials could be reduced.

The key functions of geotextiles in improving flexible pavement performance are separation, reinforcement, and filtration [1]. Unlike geotextile, the reinforcement function is the main function of geogrid for the flexible pavement. Reinforcement refers to the mechanism(s) by which the engineering properties of the composite soil/aggregate are mechanically improved [2]. Geogrid reinforcement mechanisms can be distinguished into lateral restraint, improved bearing capacity and tensioned membrane effect [3]. From these mechanisms, the lateral restraint, also known as "confinement", has been identified as the primary reinforcement mechanisms of geogrid [2] [3]. This is the ability of the aperture geometry of a grid to confine the aggregate particles within the plane of the material [3]. Hence, the geometry of geogrid aperture and the average particle size of aggregate material become important for the lateral restraint mechanism.

Since there are several types of geogrid, such as uniaxial geogrid, biaxial geogrid and triangular geogrid (also called multiaxial geogrid), lateral restraint mechanism will be different depending on the geogrid type. For the recently developed triangular geogrid, there is limited information regarding the reinforcement mechanisms. Therefore, it becomes necessary to know the reinforcement behavior of this triangular geogrid. In this study, a commercially available triangular geogrid (TX160) was selected and its reinforcement behavior was examined by conducting large scale laboratory model test. Regarding the reinforcement position in base-course layer, the optimal placement position of the geosynthetic depends on the thickness of the base-course layer and the applied load magnitude, according to S. W. Perkins [4]. Thus, current study also focused on the reinforcement position in the granular layer in order to know the optimum use of geogrid in the unbound granular layer, together with different base-course thicknesses under the cyclic loading of variable load magnitudes.

2. EXPERIMENTAL PROGRAM

In this study, seven cyclic loading tests were performed, considering base-course thickness,

geogrid reinforcement position in base-course layer and the applied stress levels. For no reinforcement, base-course thicknesses were 10 cm, 20 cm and 30 cm. In geogrid-reinforced tests, base course thicknesses were 10 cm and 20 cm. For 20 cm thick base course, the reinforcement positions were considered as the reinforcement depth ratios (a/h) of 1.0, 0.75 and 0.5 which were obtained when the depth of reinforcement (a) was divided by the base-course thickness (i.e. h = 20 cm). Test conditions are summarized in Table 1.

Table 1 Test conditions

Test ID	*BC thickness (cm)	Reinforcement	**a/h
10X	10	Non	-
20X	20	Non	-
30X	30	Non	-
10T	10	TX160	1.0
20T1.0	20	TX160	1.0
20T0.75	20	TX160	0.75
20T0.5	20	TX160	0.5

* base course

** reinforcement depth ratio

Remarks:

1) Subgrade was modelled by fine uniform sand and prepared by sand raining method.
2) BC was modelled by coarse uniform sand and prepared by compaction.
3) In each test, cyclic load was applied with varying magnitudes ranging from 100 kPa to 550 kPa (500 cycles for each loading step).

3. MATERIALS

3.1 Subgrade and Base Course

Silica Sand No.5 and No.1 were used for the model subgrade and base course preparation. These sands are commercially available in Japan. These sands were selected because they have uniform gradation, and, hence, there would be minimum variation in the particle size distribution in each test. The model subgrade sand has the following index properties: the specific gravity G_s = 2.675, the average particle size D_{50} =0.488 mm, coefficient of uniformity C_u = 1.98, coefficient of curvature C_c = 0.943, maximum dry density ρ_{max} = 1.628 g/cm^3, minimum dry density ρ_{min} = 1.338 g/cm^3. Model base course has the average particle size D_{50} of 3.735 mm, uniformity coefficient C_u of 1.904 and curvature coefficient C_c of 0.879. Since C_u and C_c values of both sands are not in the range (C_u > 6 and 1 < C_c < 3) specified by Unified Soil Classification System (USCS), they can be regarded as poorly graded sand (SP) [5]. The particle size distribution curves of these sands are presented in Fig. 1.

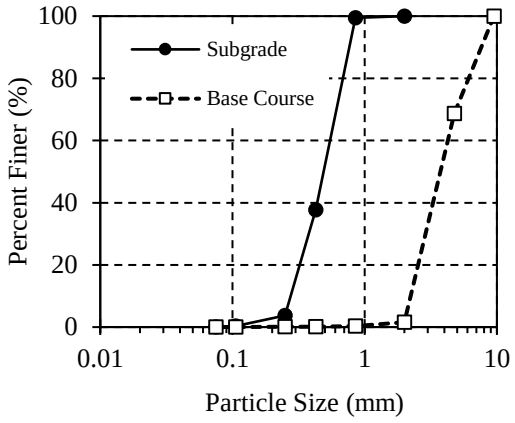

Fig. 1 Particle size distribution curves

3.2 Reinforcement Material

In this study, the commercially available triangular geogrid (trade name TX160, product of Tensar) was used for the reinforcement purpose. This geogrid has the tensile strength of 10 kN/m in the cross-machine direction and diagonal directions, pitch length of 40 mm along each side of triangular aperture, and unit weight of 245 g/m^2. The dimensions of TX160 geogrid are illustrated in Fig. 2.

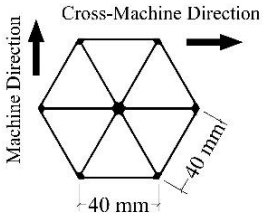

Fig. 2 Dimensions of triangular geogrid (TX160)

4. EXPERIMENTAL SETUP AND TESTING

In this experimental study, a large square container (100 cm x 100 cm x 80 cm) was used for the preparation of model pavement sections. A rigid circular steel plate, diameter = 17.5 cm, was used as a model footing. Since the total depth of subgrade and base course was greater than 70 cm in each test, the boundary influence from the tank base would be negligible according to Boussinesq Stress Distribution Analysis. In addition to this, the influences from the tank walls would be minimal on the test data because the size ratio between tank and footing diameter is considerably large (100/17.5 ≈ 6) [6] [7].

In order to model the subgrade soil, the sand raining method was adopted and used in accordance with the literatures [8] [9] [10]. A large raining box was developed so that the sand raining area covered over the plan area of tank. By using this raining

method, the relatively high density was achieved in each test, as the average of 1.6 g/cm^3. These densities were calculated from the total mass of sand and the obtained average thickness.

After subgrade layer was prepared, a small plastic plate was placed at the predefined location where subgrade deformation was monitored, directly beneath the footing. Then, a small aluminum tube was set above this plate and was hold in vertical position with the help of supporting system. After that, coarse silica sand was spread over the subgrade layer in case of no reinforcement, while geogrid was placed in case of reinforcement. After the mass of 80 kg coarse sand have been filled, the compaction was manually conducted through the wooden plate in order to minimize the breakage of material. The obtained thickness was about 5 cm as an average after compaction. The same procedure was continued until the desired base-course thickness was obtained. The experimental layout is shown in Fig 3.

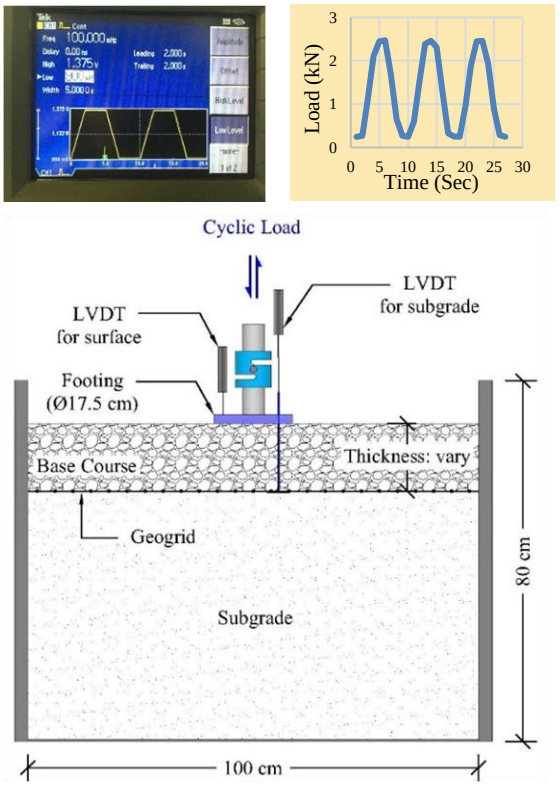

Fig.3 Experimental layout and test setup

The model footing was set after the preparation of subgrade and base course layers. A linear variable displacement transducer was set on the footing to monitor surface deformation, while another transducer was used to monitor subgrade deformation through the small aluminum tube. To simulate trafficked loading, a trapezoidal load pulse with a frequency of 0.1 Hz was applied with the help of function generator, E-P transducer and pneumatic pressure via Bellofram cylinder. The generated voltage from function generator and the resulting load pulse are shown in Fig. 3. In each test, cyclic load was applied with variable amplitudes ranging from 100 kPa to 550 kPa. Each loading step was allowed until 500 load cycles. Load and deformations at the surface and subgrade were recorded by the data acquisition system at every 1 second.

5. RESULTS AND DISCUSSION

5.1 Influence of Base Course Thickness

The influence of base-course thickness was analyzed on the surface and subgrade deformations of geogrid-stabilized sections and non-stabilized sections. These are shown in Fig.4 and Fig.5, in which the legends represent the test conditions, as presented in Table 1.

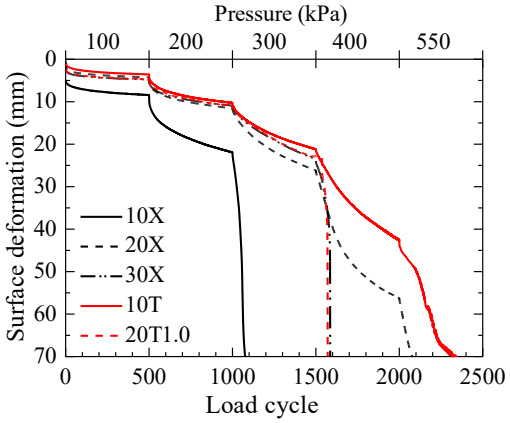

Fig.4 Influence of base-course thickness on surface deformation

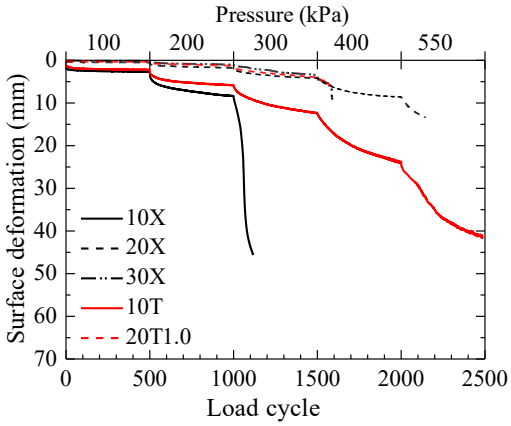

Fig.5 Influence of base-course thickness on subgrade deformation

As seen in Fig.4, the largest surface deformation was observed in the 10cm thick non-stabilized section (10X) since initial loading. Under 300 kPa pressure, this section suddenly failed just after few load cycles. This sudden deformation attributed to the bearing

capacity failure of subgrade layer, shown in Fig.5. For 10 cm thick geogrid-stabilized section (10T), the significant improvement was observed under all loading stages, and this became more obvious with the increase in the stress levels. Though the surface deformation of 10T was much smaller than that of the corresponding non-stabilized section 10X, the subgrade deformations were similar to each other under 100 kPa pressure. For this test section, the reduction in subgrade deformation was started notice under 200 kPa pressure together with load cycles, shown in Fig.5. Thus, it can be assumed that the reinforcement action of geogrid might not have been fully mobilized under 100 kPa. However, the smaller surface deformation in 10T revealed that this improvement would have been contributed from the lateral confinement action of geogrid. This also implied that the confinement action of geogrid first appeared as soon as load was applied, and the full reinforcement mobilization would have been achieved with increasing load magnitudes. For 10 cm thick base-course, the benefit of geogrid stabilization was more significant with the increase in pressure and with load cycles.

When base-course thickness was increased to 20 cm, the improvement was noticed in case of non-stabilized sections (10X and 20X in Fig.4). However, this improvement was negligible when the base course was further increased to 30 cm (30X), in which a slight improvement was observed under 300 kPa pressure. Then, this 30cm thick section suddenly failed due to the lateral flow of aggregate materials under 400 kPa pressure. For the geogrid-stabilized sections, there was no obvious improvement when the base course was increased from 10 cm to 20 cm (10T and 20T1.0). Similar to 30X test, the sudden failure was found in 20T1.0 test. That might be due to the lateral flow of aggregate materials under 400 kPa pressure, before the reinforcement action of geogrid was fully mobilized.

Regarding the behavior of subgrade deformation, the deformations were minimal in thick base-course sections: 20X, 30X and 20T1.0, regardless of geogrid-stabilized conditions. Though base-thickness was increased to 30 cm in non-stabilized section, there was no obvious reduction in subgrade deformation, compared to 20 cm thick section (20X). This might be due to the nature of uniformity of aggregate. Because of uniform characteristic of this aggregate, the internal friction angel would be small and, the resulting stress distribution angle might also be small. Qian et al. also reported that the stress distribution angle became smaller with the number of load cycle [11]. Hence, the influence of base-course thickness might have been smaller with the increasing load cycles.

Interestingly, the geogrid-stabilized section 20T1.0 behaved like 30 cm thick non-stabilized one (30X) in both surface and subgrade deformation characteristics. For the 10cm thick geogrid-stabilized section, it showed even better performance than that of 20X section, especially after 200 kPa stage. Hence, it was realized that the effect of geogrid inclusion in base-course layer was equivalent to the 10cm thickness of the given type of aggregate material. Thus, the required amount of aggregate could be reduced by mean of geogrid stabilization. Due to this aggregate uniformity, however, geogrid stabilization could be effective only in thin base course if geogrid was placed at the boundary between subgrade and base course (10T in Fig.4).

5.2 Effect of Geogrid Position in Base-Course Layer

Since a flow-type deformation was observed in 20 cm thick geogrid-stabilized base course, this thickness was selected to investigate the effect of geogrid position in the base course layer. Two more tests were performed; one with geogrid laid in the bottom-third of base course (a/h = 0.75) and the other in the middle of base course (a/h = 0.5). The surface and subgrade deformations were illustrated in Fig. 6 and Fig.7.

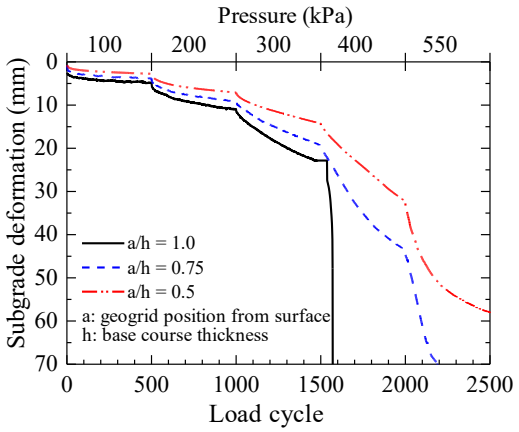

Fig.6 Surface deformation (geogrid position)

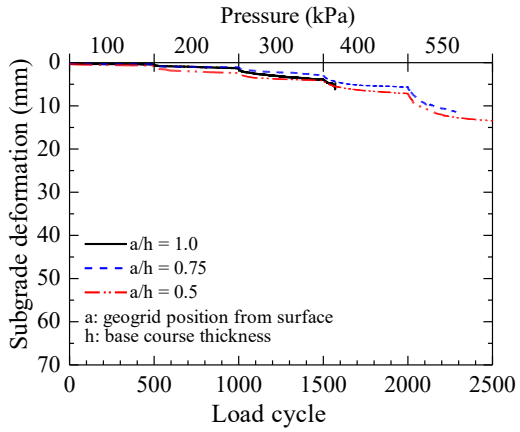

Fig.7 Subgrade deformation (geogrid position)

From Fig.6, it can be clearly seen that the surface deformation was effectively reduced at all level of loadings when a/h ratio became smaller. The improvement due to the smaller a/h ratio was more pronounced under high pressure levels (400 kPa and 550 kPa). Interestingly, the subgrade deformations were similar in these tests though there were obvious differences between the respective surface deformations. Thus, it was realized that the effect of geogrid position is insignificant on the subgrade deformation behavior.

When geogrid was placed inside base-course layer rather than above the subgrade layer, the geogrid would have confined the aggregate materials on both sides of the layer. As a result, the base course layer became stiffer and the improved bearing resistance would be achieved, sustaining until the end of 550 kPa loading stage, shown in Fig.6. In addition, the lateral flow potential of aggregate material was effectively reduced with smaller a/h ratio due to optimal confinement effect on both sides of geogrid.

5.3 Loss in Base Course Thickness

In order to investigate the benefit of geogrid stabilization, the loss in base-course thickness (*LBC*) was calculated under each pressure level. This was simply formulated considering the difference in the rates of deformation between surface and subgrade, shown in Eq. (1).

$$LBC = \sum \left(\Delta d_f - \Delta d_{sg} \right) \quad (1)$$

Where,

Δd_f : rate of surface deformation

Δd_{sg} : rate of subgrade deformation

The variation in the loss of base-course thickness is shown in Fig.8, in which the presented data were taken after 500 cycles of loading. As seen in Fig.8, the loss in base-course thickness was successfully reduced at all pressure levels with the inclusion of geogrid. In all cases, the loss in base-course thickness became more obvious with increasing pressure level. Sun et al. [12] also reported the similar behavior in their study.

When *LBC* values were compared between non-stabilized (10X) and stabilized (10T) sections, the geogrid-stabilized section reduced about 5 mm under given pressure level, though it was known that the surface deformations were attributed to the subgrade deformations in both tests. On the other hand, the non-stabilized sections: 20X (20 cm thick) and 30X (30 cm thick), and geogrid-stabilized sections: 20T1.0 (20 cm thick, a/h = 1.0) and 20T0.75 (20 cm thick, a/h = 0.75) showed similar values of *LBC* under low pressure levels (< = 200 kPa). Among these tests, the slight reductions in *LBC* were noticed with base-course thickness (20X to 30X) and geogrid position (20T1.0 to 20T0.5) under 300 kPa pressure, after which the sudden failures were observed in 30X and 20T1.0. These failures were mainly contributed from the lateral flow of aggregate materials.

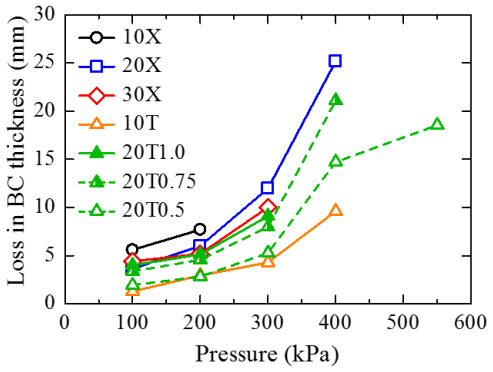

Fig.8 Loss in base-course thickness

For the geogrid stabilized sections: 10T (10 cm thick) and 20T0.5 (20 cm thick, a/h = 0.5), *LBC* values were almost same under the pressures of 100 kPa, 200 kPa and 300 kPa. However, a larger value of *LBC* was noticed in 20T0.5 than in 10T under 400 kPa pressure. This could be explained from the subgrade deformation behavior. The rate of subgrade deformation in 10T test had been progressively increased under 400 kPa pressure (10T in Fig.5). Hence, the resulting surface deformation was mainly contributed from this subgrade deformation. In addition, the large deformation in subgrade would promote to occur the tension membrane mechanism in geogrid. This behavior is good in agreement with the statement in which the tension membrane effect was recognized when permanent deformation was larger than 33% of the base thickness, reported by Qian et al. [11].

On the other hand, the subgrade deformation of 20T0.5 (a/h = 0.5 in Fig.7) was considerably small, compared to that of 10T. Thus, the potential of loss in base-course thickness of 20T0.5, due to lateral flow, was successively increased under 400 kPa pressure. This could result in a linearly increasing trend of surface deformation under 400 kPa pressure, shown in Fig.6 (a/h = 0.5). A concave trend of this curve was observed under 550 kPa pressure. This means that the rate of surface deformation became slower with load cycles, unlike the linear trend under 400 kPa. This slower rate might have been resulted from the certain progressive rate of subgrade deformation (a/h = 0.5 in Fig.7). Hence, tension membrane action would have been initiated in the geogrid together with the subgrade deformation, resulting in the larger confinement effect and in the lower rate of increase in *LBC* values, as seen in Fig.8. From these test data, it is generally realized that the loss or deterioration of

base course is mainly related to the applied stress level, and this can be effectively reduced by changing the geogrid position inside the base course layer.

6. CONCLUSIONS

The behavior of geogrid inclusion in the unbound granular layer was studied through large scale model tests. The uniform silica sands No.5 and No.1 were used as model subgrade and base-course layers. The cyclic loading with varying load magnitudes was applied through the circular rigid footing. From this study, the followings were summarized as:

(1) For the given type of granular material, the effective improvement due to geogrid-stabilization was observed in thin base-course section, if geogrid was placed at the boundary between subgrade and base-course layer.
(2) The surface and subgrade deformations were optimally reduced with the geogrid stabilization. However, this reduction was insignificant with the increase in base-course thickness.
(3) In thin base-course section, surface deformation was mainly contributed from the subgrade deformation, while lateral flow dominated in thick section.
(4) Flow type deformation was obviously minimized with the smaller reinforcement depth ratios. The optimum depth was known when geogrid was laid at the middle of base course.
(5) The influence of reinforcement position was negligible on the subgrade deformation behavior.
(6) Loss in base-course thickness (*LBC*) or base course deterioration is smaller in the thinner base course, while this is larger in thick section. This *LBC* can be successfully minimized with the smaller reinforcement depth ratios.
(7) In all tests, the increase in *LBC* was noticed with increasing pressure levels.

7. ACKONWLEDGEMENTS

This study was collaborated with NIPPO CORPORATION and MITSUI CHEMICALS INDUSTRIAL PRODUCTS LTD. Their supports are highly appreciated.

8. REFERENCES

[1] I. L. Al-Qadi, T. L. Brandon, R. J. Valentine, B. A. Lacina and T. E. Smith, "Laboratory Evaluation of Geosynthetic-Reinforced Pavement Sections," *Transportation Research Record*, issue 1439, pp. 25-31, September 1994.

[2] R. P. Anderson, "Geogrid Separation," in *Proceedings of International Conference on New Developments in Geoenvironmental and Geotechnical Engineering*, Incheon, Republic of Korea, 2006.

[3] Stephen Archer, P.E., "Subgrade Improvement for Paved and Unpaved Surfaces Using Geogrids," CE News Professional Development Hours, 2008.

[4] S. W. Perkins, "Mechanical Response of geosynthetic-reinforced flexible pavements," *Geosynthetics International*, vol. 6, no. 5, pp. 347-382, 1999.

[5] J.-P. Bardet, Experimental Soil Mechanics, Upper Saddle River, New Jersey: Prentice-Hall Inc., 1997.

[6] H. A. Alawaji, "Settlement and bearing capacity of geogrid-reinforced sand over collapsible soil," *Geotextiles and Geomembranes*, vol. 19, pp. 75-88, 2001.

[7] T. Yetimoglu, J. T. H. Wu and A. Saglamer, "Bearing Capacity of Rectangular Footings on Geogrid-Reinforced Sand," *Journal of Geotechnical Engineering, ASCE*, vol. 120, no. 12, pp. 2083-2099, December 1994.

[8] S. Miura and S. Toki, "A sample preparation method and its effect on static and cyclic deformation-strength properties of sand," *Soils and Foundations*, vol. 22, no. 1, pp. 61-77, March 1982.

[9] Y. P. Vaid and D. Negussey, "Technical Note: Relative density of pluviated sand samples," *Soils and Foundations*, vol. 24, no. 2, pp. 101-105, 1984.

[10] T. N. Dave and S. M. Dasaka, "Assessment of portable travelling pluviator to prepare reconstituted sand specimens," *Geomechanics and Engineering*, vol. 4, no. 2, pp. 79-90, 2012.

[11] Y. Qian, J. Han, S. K. Pokharel and R. L. Parsons, "Performance of Triangular Aperture Geogrid-Reinforced Base Courses Over Weak Subgrade under Cyclic Loading," *Journal of Materials in Civil Engineering*, vol. 25, no. 8, pp. 1013-1021, August 2013.

[12] X. Sun, J. Han, J. Kwon, R. L. Parsons and M. H. Wayne, "Radial stresses and resilient deformations of geogrid-stablized unpaved roads under cyclic plate loading tests," *Geotextiles and Geomembranes*, vol. 43, no. 5, pp. 440-449, 10 2015.